Paper 103

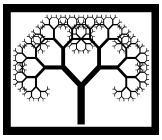

Proceedings of the Eleventh International Conference
on Computational Structures Technology,
B.H.V. Topping, (Editor),
Civil-Comp Press, Stirlingshire, Scotland

The Non-Linear Influence of Ballast on the Vibrations of Railway Bridges

J.-M. Battini
Division of Structural Engineering and Bridges
KTH Royal Institute of Technology, Stockholm, Sweden

Abstract

In numerical dynamic analyses of railway bridges, the ballast is either considered as an additional mass or modeled using a mass-spring-damper system between the bridge deck and the sleepers. In both cases, the influence of the ballast on the natural frequencies of the bridge is neglected. However, a research project at the Division of Structural Engineering and Bridges at KTH has shown that the ballast may influence significantly the first natural frequency of bridges. To consider that aspect, a new finite beam element model has been developed. The main feature of the element is that the effect of the ballast is introduced through a non-linear longitudinal stiffness associated to the slip at the interface between the bridge and the ballast. This simple element can be used to model accurately the vertical vibrations in bridges, which allows a better prediction of the fatigue life.

Keywords: railway bridges, dynamic analyses, finite elements, ballast.

1 Introduction

Static analyses are often used to estimate the fatigue life for railways bridges. However, dynamic analyzes may be necessary in order to obtain a more accurate estimation. In particular, a recent research at the Division of Structural Engineering and Bridges at KTH has shown that the free vibrations of bridges after the train passage may influence the fatigue life. One issue regarding the dynamic behavior of railway bridges is that discrepancies between calculations and experiments are often observed. This problem especially applies to short or median span bridges for which important differences between calculated and measured natural frequencies can be obtained. Several studies, see e.g. [1] and [2], have also shown that, for such bridges, the natural frequencies vary as function of the amplitude of vibration.

One difficulty in modeling relatively short railway bridges is that the influence of the track superstructure composed by rails, sleepers and ballast is not well known. As example, there is, so far, no clear recommendation in design codes to take the ballast into account in dynamic analyzes. In several works about train-track-bridge dynamic interaction [3, 4, 5, 6], the track and the bridge have been modeled by two beams and the effect of the ballast has been introduced using a more or less advanced system of viscoelastic spring/dampers and masses between the two beams. In [7], Liu et al. developed a 3D finite element model of the bridge using elastic solid elements for the ballast. Müller et al. [8] and Ruge et al. [9, 10] developed a truss model to study the longitudinal stresses due to temperature changes and train braking. Following the European codes, they introduced a non-linear stiffness between the bridge and the rail to represent the coupling effect of the ballast.

The purpose of the present article is to propose a new and simple approach to model the effect of the ballast in vertical dynamic analyses of railway bridges. The idea is to use the methodology in [8, 9, 10] to develop a simple 2D beam finite element. In this element, the effect of the ballast is taken into account by introducing a linear or non-linear longitudinal stiffness associated to the slip at the interface between the bridge and the ballast. This approach has already been presented by Fink and Mähr [11], but in a continuum context, using differential equations. The organization of the paper is as follow: the derivation of the finite element is presented in Section 2. In Section 3 and 4, two numerical applications, based on lab and in-situ experiments are proposed. In particular, it is shown that the present element can be used to model the variation of the lowest bending natural frequency as function of the amplitude of vibration. Finally, conclusions are presented in Section 5.

2 Finite element formulation

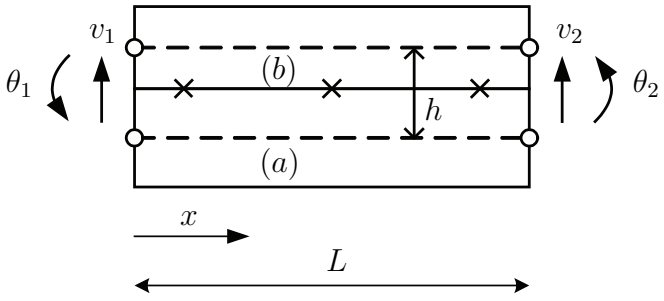

Figure 1: Element kinematics

The finite element, see Figures 1 and 2, consists of two layers. The layer (a) represents the bridge whereas the layer (b) represents the track superstructure composed by rails, sleepers and ballast. The slip at the interface between the two layers is considered. The element has four degrees of freedom. The horizontal displacements of

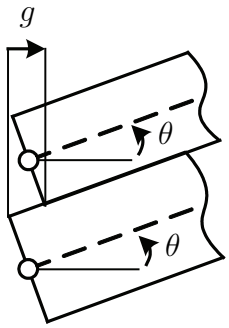

Figure 2: Slip at the interface

the neutral axes of the two layers are not considered. It is assumed that the vertical displacements v and rotations θ of the neutral axis of the two layers are the same. The Bernoulli hypothesis is adopted, together with cubic shape functions, which gives

$$\theta(x) = \frac{\partial v}{\partial x} = v' \tag{1}$$

$$v(x) = f_1(x)v_1 + f_2(x)\theta_1 + f_3(x)v_2 + f_4(x)\theta_2 \tag{2}$$

with

$$f_1(x) = 1 - 3\left(\frac{x}{L}\right)^2 + 2\left(\frac{x}{L}\right)^3 \tag{3}$$

$$f_2(x) = x\left(1 - \frac{x}{L}\right)^2 \tag{4}$$

$$f_3(x) = 3\left(\frac{x}{L}\right)^2 - 2\left(\frac{x}{L}\right)^3 \tag{5}$$

$$f_4(x) = \frac{x^2}{L}\left(\frac{x}{L} - 1\right) \tag{6}$$

The bending strain and kinetic energy in the element are calculated by

$$\phi_{bs} = \frac{1}{2}\left(E_a I_a + E_b I_b\right) \int_L (v'')^2 \, \mathrm{d}x \tag{7}$$

$$\phi_k = \frac{1}{2}\left(\rho_a A_a + \rho_b A_b\right) \int_L (\dot{v})^2 \, \mathrm{d}x \tag{8}$$

where E_i, A_i, ρ_i and I_i are the elastic modulus, the area, the density and the second moment of area of the layer cross-section i.

This gives the classical stiffness and mass matrices as

$$\mathbf{k} = \frac{EI}{L^3} \begin{bmatrix} 12 & 6L & -12 & 6L \\ 6L & 4L^2 & -6L & 2L^2 \\ -12 & -6L & 12 & -6L \\ 6L & 2L^2 & -6L & 4L^2 \end{bmatrix} \tag{9}$$

$$\mathbf{m} = \frac{\rho AL}{420} \begin{bmatrix} 156 & 22L & 54 & -13L \\ 22L & 4L^2 & 13L & -3L^2 \\ 54 & 13L & 156 & -22L \\ -13L & -3L^2 & -22L & 4L^2 \end{bmatrix} \tag{10}$$

with

$$EI = E_a I_a + E_b I_b \quad \rho A = \rho_a A_a + \rho_b A_b \tag{11}$$

As shown in Figures 1 and 2, the slip g at the interface between the bridge and the ballast is obtained as

$$g = h\,\theta \tag{12}$$

which, introducing Equations (1) to (6), gives

$$g = h\,\mathbf{G}\,\mathbf{d} \tag{13}$$

with

$$\mathbf{G} = \begin{bmatrix} f_1'(x) & f_2'(x) & f_3'(x) & f_4'(x) \end{bmatrix} \tag{14}$$

and

$$\mathbf{d} = \begin{bmatrix} v_1 & \theta_1 & v_2 & \theta_2 \end{bmatrix}^{\mathrm{T}} \tag{15}$$

The effect of the ballast is modeled by a shear force F at the interface. This force is taken as a non-linear function of the slip g. Following Müller et al. [8] and Ruge et al. [9, 10], a bilinear law is adopted. It is shown in Figure 3 and defined by

$$F = F(g) \qquad C = \frac{\partial F}{\partial g} \tag{16}$$

It can be observed that F is the resultant of the forces acting through the width of the interface and along a unit length. F is therefore in N/m.

The internal forces $\mathbf{f}$ at the nodes which give the same virtual work as the force F in the element are defined by

$$\delta\mathbf{d}^{\mathrm{T}}\mathbf{f} = \int_L \delta g^{\mathrm{T}} F \,\mathrm{d}x \tag{17}$$

which, by introducing Equation (13), gives

$$\mathbf{f} = h \int_L \mathbf{G}^{\mathrm{T}} F \,\mathrm{d}x \tag{18}$$

The corresponding tangent stiffness matrix, defined by

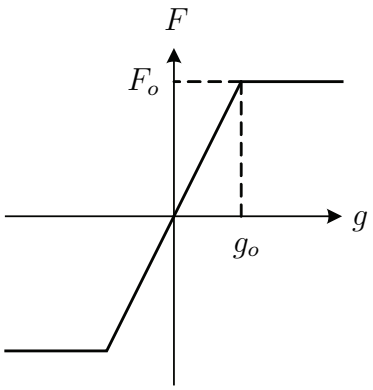

Figure 3: Bilinear shear force-slip law

$$\delta\mathbf{f} = \mathbf{k}_t\,\delta\mathbf{d} \tag{19}$$

is obtained from Equations (13), (16), (18) and (19) as

$$\mathbf{k}_t = h^2 \int_L \mathbf{G}^{\mathrm{T}} C\,\mathbf{G}\,\mathrm{d}x \tag{20}$$

$\mathbf{f}$ and $\mathbf{k}_t$ are calculated using three Gauss points along the length of the element (the positions of the Gauss points are indicated by $\times$ in Figure 1). It can be noted that $\mathbf{G}$ consists of polynomials of second order and consequently an exact integration is obtained if C is constant and taken as

$$C = \frac{F_o}{g_o} \tag{21}$$

which means that only the linear part in Figure 3 is considered. In that case, the tangent stiffness matrix is constant and is obtained as

$$\mathbf{k}_{tc} = \frac{C\,h^2}{30L}\begin{bmatrix} 36 & 3L & -36 & 3L \\ 3L & 4L^2 & -3L & -L^2 \\ -36 & -3L & 36 & -3L \\ 3L & -L^2 & -3L & 4L^2 \end{bmatrix} \tag{22}$$

Finally, the free vibrations of the composite beam are expressed by the non-linear equation

$$f(\mathbf{d}, \ddot{\mathbf{d}}) = \mathbf{m}\,\ddot{\mathbf{d}} + \mathbf{f} + \mathbf{k}\,\mathbf{d} = 0 \tag{23}$$

with

$$\ddot{\mathbf{d}} = \begin{bmatrix} \ddot{v}_1 & \ddot{\theta}_1 & \ddot{v}_2 & \ddot{\theta}_2 \end{bmatrix}^{\mathrm{T}} \tag{24}$$

Equation (23) is solved step by step using the average acceleration method. For that, the expression

$$\frac{\partial f}{\partial \mathbf{d}} = \mathbf{k}_t + \mathbf{k} \tag{25}$$

is needed.

The purpose of the present work is to study the free vibrations of the lowest bending modes separately. Therefore the initial value of the displacement vector $\mathbf{d}$ (or the acceleration vector $\ddot{\mathbf{d}}$) is taken as the bending mode and is calculated by an eigenvalue analysis of Equation (23) in which the non-linear term $\mathbf{f}$ is replaced by the linear term

$$\mathbf{k}_{tc}\,\mathbf{d} \tag{26}$$

The initial nodal velocities are taken to zero. By doing that, the vibration of the bridge is harmonic with the bending mode as shape. Using these initial conditions, the response of the structure is calculated by using time integration and the natural frequency is obtained by considering the times at which the displacements are maximum. Then, by taking different initial amplitudes it is possible to study the variation of the lowest natural frequencies in bending.

3 Example 1 - Experimental bridge

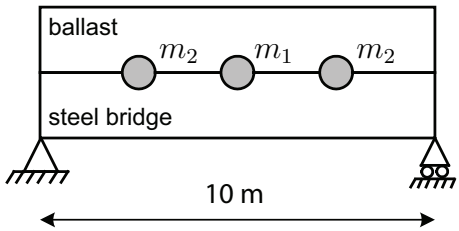

Figure 4: Experimental bridge - model

Bridge	$E_a I_a = 1.1631 \cdot 10^8$ Nm^2
	$\rho_a A_a = 635$ kg/m
	$m_1 = 3193$ kg
	$m_2 = 481$ kg
Ballast	$E_b I_b = 1.2831 \cdot 10^7$ Nm^2
	$\rho_b A_b = 3099$ kg/m

Table 1: Experimental bridge - data

The first application is the experimental steel bridge developed and tested by Fink and Mähr at the Technical University of Vienna [11]. The main interest of this experiment is that it shows clearly that the ballast has an influence on the mechanical properties of the bridge and cannot be considered just as an additional mass.

max ampl. ($\times 10^{-5}$) m	175	302	407	489	532
measured freq. (Hz)	4.32	4.08	3.95	3.87	3.84
calculated freq. (Hz)	4.27	4.18	3.97	3.84	3.77

Table 2: Experimental bridge - results

The bridge, see Figure 4 and Table 1, has two main girders consisting of two HEA beams. The bridge deck is made of timber beams and panel. The bending stiffness ($E_a I_a$) of the bridge is taken as the ones of the two HEA girders. The track superstructure consists of a 55 cm thick ballast bed, reinforced concrete sleepers and two UIC 60 rails. The bending stiffness of the track superstructure ($E_b I_b$) is taken as the one of the two UIC 60 rails, which means that it is assumed that bridge and the rails have the same kinematics. The mass of the track superstructure ($\rho_b A_b$) includes the ballast, the rails and the sleepers. The modal properties of the bridge were measured using a system of two eccentric weight vibration generators inducing a harmonic force. m_1 and m_2 are the mass of the framework and generator at midspan and the mass of the framework at the first and third quarter. The bridge has been modeled using 8 beam elements.

The bridge was first tested without the ballast superstructure. Two tests, with different eccentric weights, were performed. Both tests gave the same first resonance frequency, 4.66 Hz. This shows that without the ballast the bridge has a linear behavior. The calculated first natural frequency is 4.58 Hz. It can then be concluded that the numerical model of the bridge is accurate.

The bridge was then tested with the ballast superstructure. Several tests, with different eccentric weights, were performed. In each test, the resonance appears at a different frequency, in the range of 3.84 Hz and 4.32 Hz. The measured resonance frequencies and the maximum midspan amplitudes at resonance are given in Table 2. The first natural frequency calculated by introducing only the stiffness of the rails ($E_b I_b$) and the mass of ballast superstructure ($\rho_b A_b$) is 2.66 Hz. These experimental and numerical results show that the ballast introduces additional stiffness and that this additional stiffness is not constant but depends on the amplitudes of the vibration.

The bilinear shear force-slip law between the ballast and the bridge has then been added in the numerical model. Equation (23) has been solved by taking as initial displacement the first calculated eigenmode with the five maximum midspan amplitudes observed in the tests. In each case, the first natural frequency has been calculated from the numerical solution of Equation (23) (free vibration response). The parameters g_o and F_o have been calibrated so that the difference between the 5 measured and the 5 calculated frequencies is as small as possible. For that, the MATLAB function fminsearch has been used. The results shown in Table 2 have been obtained with

$$g_o = 7.30 \cdot 10^{-4}\,\text{m} \quad F_o = 1.45 \cdot 10^{4}\,\text{N/m} \tag{27}$$

Very good agreement between the measurements and the numerical model can be observed. The largest difference, obtained with a measured frequency of 4.08 Hz, is

only 2.4 %.

It can also be observed that the obtained values are of the same magnitude as the ones given in [9, 10] ($g_o = 2 \cdot 10^{-3}$ m, $F_o = 2 \cdot 10^4$ N/m for unloaded ballasted track in summer). However, it is not certain that a comparison is relevant since the values in [9, 10] are used for static analyzes of horizontal temperature effects.

Finally, the idea of the proposed approach is to consider the ballast superstructure as a beam. Then, the additional stiffness due to the ballast is introduced only through a shear force at the interface between the ballast and the bridge. Since the ballast is considered as a beam, another alternative to introduce additional stiffness is to consider some bending stiffness in the ballast beam. However, using this alternative, one must increase the total bending stiffness of the system ($E_a I_a + E_b I_b$) from $1.3 \cdot 10^8$ Nm^2 to $3.3 \cdot 10^8$ Nm^2 in order to obtain a natural first frequency of 4.27 Hz. It is clear that the ballast cannot give such additional bending stiffness and consequently this alternative is not realistic.

4 Example 2 - Composite bridge

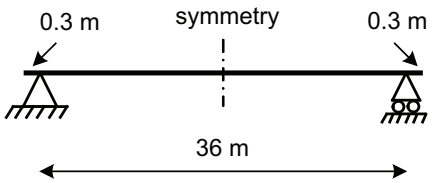

Figure 5: Composite bridge - model

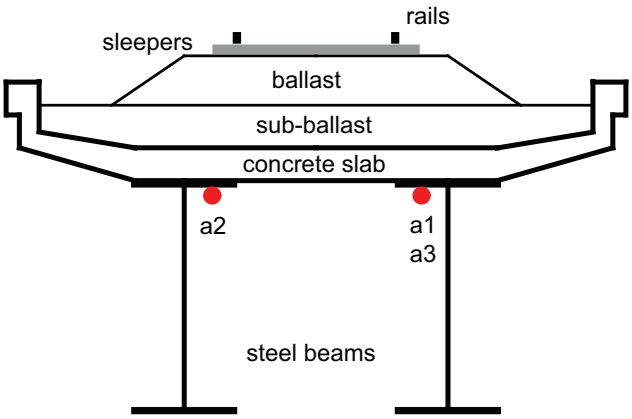

Figure 6: Composite bridge - cross-section

The bridge at Skidträsk (see Figures 5 and 6) is a single span, concrete-steel composite bridge carrying one ballasted track. Its span is 36 m. The rails are supported

Elements	L (m)	A_a (m^2)	I_a (m^4)	ρ_a (kg/m^3)
1	0.3	0.3662	0.3852	21645
2	0.25	0.3662	0.3852	21645
$3-7$	0.75	0.3564	0.3154	22023
$8-11$	1	0.4042	0.3424	20337
$12-15$	1	0.4744	0.3840	18490
$16-21$	1	0.5042	0.3958	17932

Table 3: Composite bridge - data

by concrete sleepers separated with a regular distance of 65 cm. These sleepers lie on ballast composed of rock particles with a diameter around 5 cm. The depth of the ballast layer is approximately 50 cm. The sub-ballast, composed by particles with a diameter around 10 cm, has a depth of 50 cm. A reinforced concrete slab transfers the load from the track to two main steel beams. The total width of the slab is 6.7 m and its height varies between 30 and 40 cm. The steel beams are simply supported with respect to vertical bending moments. The line of supports is skewed relative to the longitudinal axis of the track.

The bridge has been modeled using 42 beam elements. The equivalent steel section parameters ($E_a = 210$ GPa) are given in Table 3 for the 21 first elements, starting from the left side. The properties of the additional elements are obtained by symmetry. These properties have been calculated by considering a cracked concrete section. The bending stiffness of the track superstructure ($E_b I_b = 1.2831 \cdot 10^7$ Nm^2) is taken as the one of the two UIC 60 rails. The cross-section area and density of the ballast are 4 m^2 and 2040 kg/m^3, which, by adding the contribution of the rails gives $\rho_b A_b = 8280$ kg/m.

The bridge has been instrumented to measure the vertical bridge deck acceleration during and after the passage of trains. Three accelerometers situated at midpoint (a1 and a2) and at quarter-point (a3) has been used, see Figure 6.

This study is based on the free vibration of the bridge just after the passage of a freight train at the speed of about 100 km/h. In order to determine the first natural frequency in bending an average acceleration, defined by

$$a_v = \frac{a_1 + a_2}{2} \tag{28}$$

has been computed. A lowpass digital Butterworth filter has then been applied in order to remove the contribution of the other modes. The results are shown in Figure 7. These results have been used to study the influence of the amplitudes of the vibrations on the lowest natural frequency. The following method has been used: at each maximum value of the average acceleration, a corresponding natural frequency has been calculated by using the maximum values before and after (see Figure 8):

$$f(a_{vi}) = \frac{1}{t_{i+1} - t_{i-1}} \tag{29}$$

The first maximum points of the average acceleration diagram have not been used, firstly because these amplitudes are affected by the filter, secondly because it is not certain that these accelerations have been registered after the passage of the train.

The results are presented in Figure 9. It can be observed that the first natural frequency in bending increases from 3.3 Hz to 3.85 Hz when the acceleration decreases from 0.26 m/s^2 to 0.03 m/s^2.

The first natural frequency calculated without introducing the bilinear shear force-slip law is 2.63 Hz, which is quite far from the experimental results. The shear force between the bridge and the ballast has then been introduced in the numerical model. The calibration has been performed using the same method as in the first example. Five maximum amplitudes and corresponding natural frequencies have been taken from Figure 9. In each case, Equation (23) has been solved by taking as initial acceleration the first calculated eigenmode with the maximum amplitude. The first natural frequency has been calculated from the numerical solution of Equation (23). The parameters g_o and F_o have been calibrated so that the difference between the measured and the calculated frequencies is as small as possible. For that, the MATLAB function fminsearch has been used. The results shown in Table 4 has been obtained with

$$g_o = 2.103 \cdot 10^{-5}\,\text{m} \quad F_o = 6685\,\text{N/m} \tag{30}$$

Very good agreement between the measurements and the numerical model can be observed. The largest difference, obtained with an acceleration of 0.03 m/s^2, is only 1.3 $\%$.

measured acc. (m/s^2)	0.03	0.10	0.19	0.23	0.26
measured freq. (Hz)	3.84	3.75	3.60	3.46	3.30
calculated freq. (Hz)	3.79	3.79	3.60	3.42	3.32

Table 4: Composite bridge - first natural frequency

The second and third natural frequencies in bending have been also identified from the records of the three accelerometers. However, the amplitudes of the corresponding modes were too low to study the dependency between the natural frequencies and the amplitudes. Therefore linear eigenvalues computations have been performed by using the constant matrix in Equation (22). Three calculations have been performed. The results are presented in Table 5. In the first calculation, the shear force at the interface bridge/ballast is not considered. It can be observed that the computed first natural frequency is not accurate but the computed second and the third frequencies are closed to the measured one. In the second calculation, the shear force at the interface has been introduced by taking the parameters g_o and f_o obtained from the minimisation procedure. Accurate results are obtained. It can be observed that the shear force has a strong influence on the first natural frequency but only a slight influence on the second and third ones. In the third calculation, the shear force is not considered and the total bending stiffness of the system ($E_a I_a + E_b I_b$) has been multiplied by 2.05 in order to obtain the first natural frequency measured with low amplitudes. It can be observed

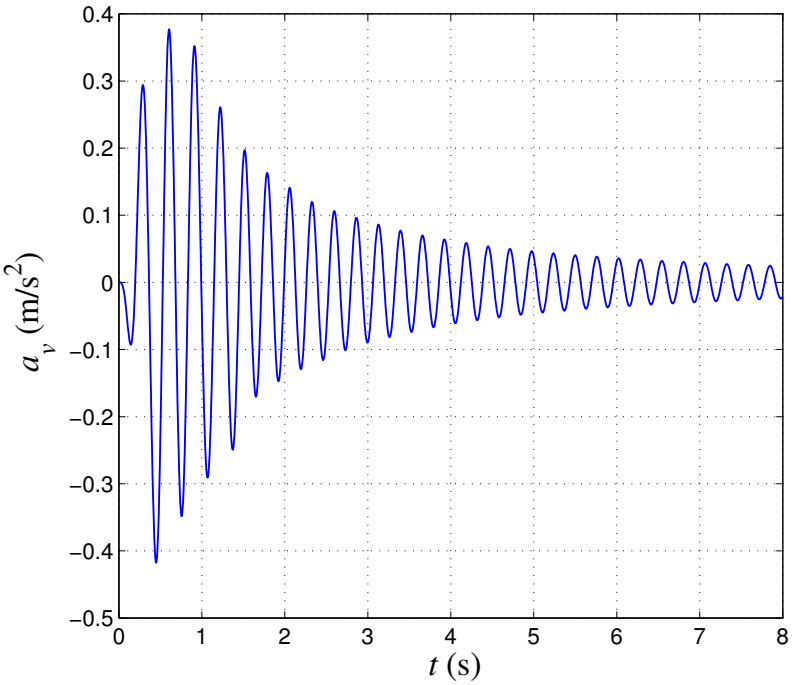

Figure 7: Composite bridge - average acceleration after filtering

that such a model is not appropriate, firstly because it is not realistic that the ballast can give such an additional stiffness, secondly because the calculated second and third frequencies are far from the measured ones.

measured frequencies	3.3-3.8	11	23
case 1 $C = 0$	2.63	10.4	23.2
case 2 $C = 6685/2.103 \cdot 10^{-5}$	3.79	11.7	24.6
case 3 $C = 0$ $(E_a I_a + E_b I_b) \times 2.05$	3.77	14.8	33.2

Table 5: Composite bridge - linear natural frequencies

Finally, in the first example, the experimental bridge has been tested with and without ballast and thereby the contribution of the ballast could be clearly identified. This was not the case for the Skidträsk bridge and therefore the above study presents certain uncertainties concerning the numerical model. The skew has not been considered. However, the bridge is rather long and the effect of the skew is therefore not important. The equivalent steel stiffness in Table 3 have been calculated by considering a cracked concrete section, which can be questioned. However, calculation using an uncracked section gives a first natural frequency of 2.80 Hz (instead of 2.63 Hz), which is still far from the experimental values (3.3Hz - 3.8 Hz). The bridge is simply supported, but the continuity of the ballast and the rails may introduce end moments at the supports.

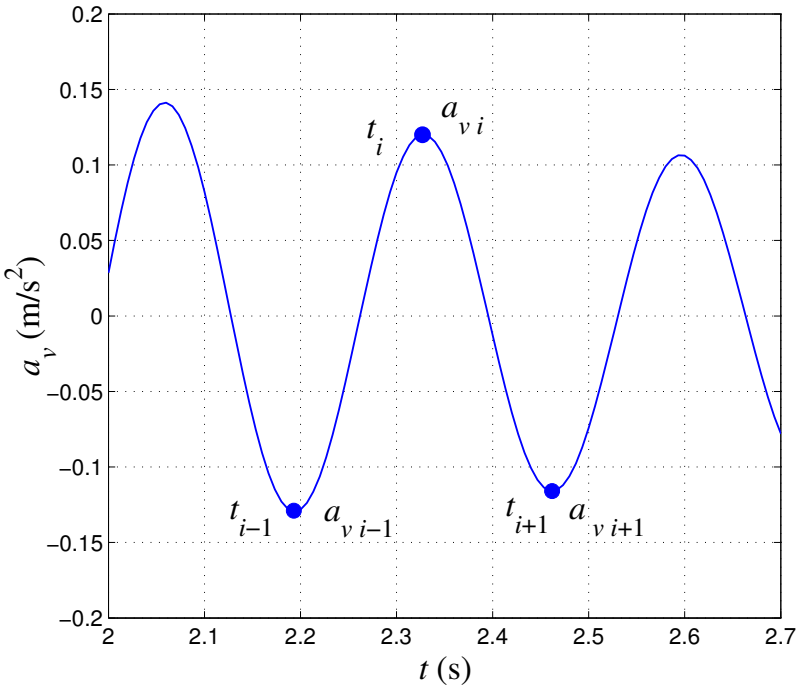

Figure 8: Composite bridge - computation of the first natural frequency

This effect has not been considered.

5 Conclusion

In this paper, a new and simple 2D beam finite element which considers the effect of the ballast on vibrations of railway bridges has been presented. The idea is to introduce a stiffness associated to the slip between the bridge and the track superstructure. This stiffness can be considered as linear or non-linear. For the non-linear case, a bilinear law has been adopted.

This model has been used in two numerical applications to study the influence of the ballast on the lowest bending natural frequencies of bridges. Very good agreement with experiments has been obtained. In particular, it has been shown that the model can catch the influence of the amplitudes of vibrations on the value of the lowest bending natural frequency.

It is clear that additional experimental and numerical studies are required in order to fully validate the proposed finite element model. One issue is to check if a bilinear law is enough or if a more advanced non-linear model is required. Another issue is to considered the additional damping due to the ballast. Finally, this model is currently used to get a better estimation of the dynamic response of the Skidtrsk bridge due to

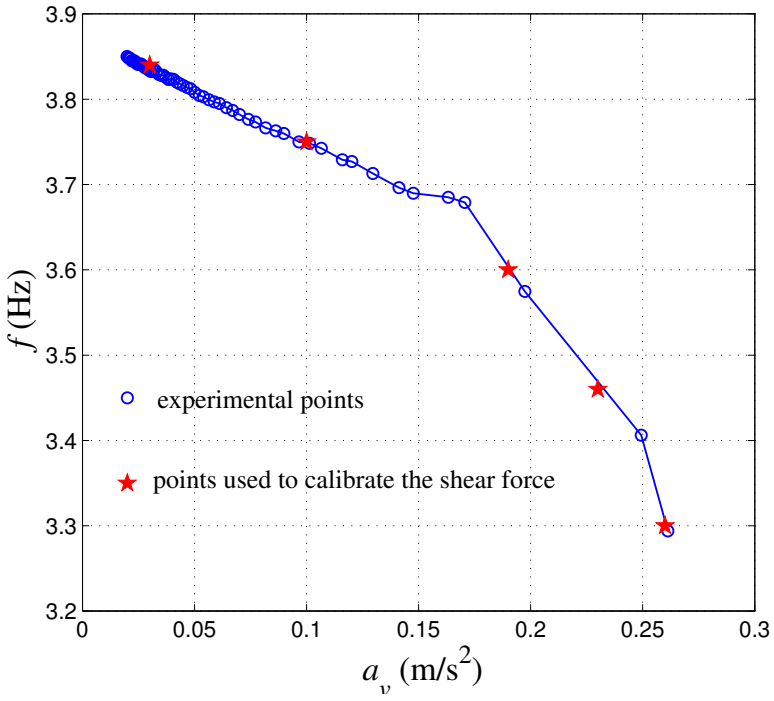

Figure 9: Composite bridge - variation of the first natural frequency

the passage of trains, and consequently a better estimation of the fatigue life.

References

[1] C. Rebelo, L. Simoes da Silva, C. Rigueiro and M. Pircher. Dynamic behaviour of twin single-span ballasted railway viaducts-Field measurements and modal identification. Engineering structures Vol 30, pp. 2460-2469, 2008.

[2] lker-Kaustell, M. and Karoumi, R. The application of the continuous wavelet transform on the free vibrations of a steel-concrete composite railway bridge. Engineering structures Vol 33, pp. 911919, 2011.

[3] B. Biondi, G. Muscolino and A. Sofi. A substructure approach for the dynamic analysis of train-track-bridge system. Computers and structures Vol 83, pp. 2271-2281, 2005.

[4] C. Rigueiro, C. Rebelo, L. Simoes da Silva. Influence of ballast models in the dynamic response of railway viaducts. Journal of Sound and Vibration Vol 329, pp. 3030-3040, 2010.

[5] Y.-S. Wu and Y.-B. Yang. Steady state response and riding comfort of trains moving over a series of simply supported bridges. Engineering structures Vol 25, pp. 251-265, 2003.

[6] J.-D. Yau, Y.-B. Yang and S.-R. Kuo. Impact response of high speed rail bridges and riding comfort of rail cars. Engineering structures Vol 21, pp. 836-844, 1999.

[7] K. Liu, E. Reynders, G. De Roeck and G. Lombaert. Experimental and numerical analysis of a composite bridge for high-speed trains. Journal of Sound and Vibration Vol 320, pp. 201-220, 2009.

[8] G. Müller, D. Jovanovic and P. Haas. Tracks-gravel-bridge interaction. Computers and structures Vol 13, pp. 607-611, 1981.

[9] P. Ruge and C. Birk. Longitudinal forces in continuously welded rails on bridgedecks due to nonlinear track-bridge interaction. Computers and structures Vol 85, pp. 458-475, 2007.

[10] P. Ruge, D.R. Widarda, G. Schmlzlin and L. Bagayoko. Longitudinal track-bridge interaction due to a sudden change of coupling interface. Computers and structures Vol 87, pp. 47-58, 2009.

[11] J. Fink and T. Mähr. Influence of ballast superstructure on the dynamics of slender railway bridge. Nordic Steel Construction Conference, 2009. http://www.nordicsteel2009.se